



Assessing Carbon Flux Variability in an Alpine Steppe: Insights from Dual-Height Measurements

Nithin D Pillai^{1,2}, Christian Wille¹, Felix Nieberding³, Manuel Helbig¹, and Torsten Sachs^{1,4}

5 ¹GFZ Helmholtz Centre for Geosciences, Telegrafenberg, 14473 Potsdam, Germany.

²Institute of Geosystems and Bioindication, Technische Universität Braunschweig, Braunschweig, Germany.

³Agrosphere Institute (IBG-3), Forschungszentrum Jülich, Wilhelm-Johne-Str., 5242, Jülich, Germany.

⁴Institute of Geoecology, Technische Universität Braunschweig, Braunschweig, Germany

10 **Correspondence to:** Nithin D Pillai (nithin.pillai@gfz.de) and Torsten Sachs (torsten.sachs@gfz.de)

Abstract

Future projections of climate warming on the Tibetan plateau (TP) imply a 4°C warming in the next 100 years, the largest in the middle of the troposphere. Climatic variabilities of this magnitude are likely to trigger a cascade of climate-carbon (C) feedbacks within the TP ecosystems. However, a robust consensus of the feedback mechanisms and their drivers is scarce due to a lack of observations and unaccounted spatial heterogeneity. In the present study, we investigated how coarse-scale heterogeneity impacts the CO₂ fluxes using a dual eddy covariance tower system (3 m and 19 m) over an alpine steppe ecosystem near the Nam Co Station for Multi-sphere Observation and Research (NAMORS) on the central TP. The source area of the 3 m height is relatively homogenous. On the other hand, the source area of the 19 m height covers the steppe and part of the neighboring lake. The steppe acted as carbon neutral over the 10-month measurement period (August 2018- May 2019) at the 19 m footprint as opposed to the 10-month long-term (2006-2018) average (-78 g C m⁻²) observed at the 3 m footprint. We found that the difference in the magnitude of CO₂ fluxes observed from the two towers was attributed to the combined effects of winter snow cover and lake-land interactions. The extreme snow accumulation over the period increased the ecosystem respiration thus elevating the emissions in winter, highlighting the role of extreme snow events in regulating carbon dynamics in high-altitude ecosystems. Additionally, the neighboring lake substantially influenced carbon fluxes over larger spatial footprints, serving as a natural buffer that mitigates land carbon emissions during critical periods. Fluxes measured from land-dominated areas at both tower heights were largely consistent, demonstrating the reliability of steppe-derived flux measurements across 3 m and 19 m footprints. The findings emphasize the critical need for adopting a landscape-scale perspective to better capture flux variability in heterogeneous environments.

Keywords: Eddy covariance, Carbon flux, Net ecosystem exchange, Snow cover, Tibetan Plateau



35 **1 Introduction**

Carbon sinks on land are considered to be the most uncertain component of the global carbon budget by far (Piao et al., 2019). A slight imbalance between the terrestrial carbon fluxes (photosynthesis and respiration) leads to significant interannual variations in atmospheric CO₂ and may have feedback effects on climate change (Meeran et al., 2021). The physical, chemical, and biological processes change at different scales due to the changing
40 interplay of processes and influencing factors at each scale. Studying the variability of carbon fluxes at various spatial scales, not only characterizes the type of terrestrial ecosystems but also provides a ‘natural experiment’ that can help the scientific community understand the complex interactions and relationships between the meteorological variables and the terrestrial ecosystems. Despite, being in one of the most extreme environmental conditions on Earth, alpine grasslands play a vital role in the exchange of water, energy, and carbon (Liu et al.,
45 2024). The Tibetan Plateau (TP) presents the world's largest alpine vegetation distribution area (Wang et al., 2021) and the alpine steppe makes up around 38.9 % of its total grassland area (Lu et al., 2015). The high root/shoot ratio, soil organic carbon, and carbon sequestration potential within a short time make steppe ecosystems an important contributor to the “missing sink” (i.e., the unknown fate of the CO₂ emissions to the atmosphere) (Gilmanov et al., 2003). Studying the carbon and energy fluxes over the water-limited alpine steppe is crucial for
50 producing regional-scale climate information to support decision-making and distillation (the process of synthesizing information about climate change from multiple lines of evidence).

The eddy covariance (EC) technique is the direct and most accurate method available to date for measuring exchanges of heat, mass, and momentum between the surface and the overlying atmosphere. The availability of EC-based carbon flux observations accelerated the research on spatial dynamics of the biogeochemical processes.
55 By offering high-resolution, direct measurements of carbon fluxes, EC observations have enabled more detailed and accurate analysis of these dynamics and their interactions with climate. The behaviour of a particular ecosystem to act as a potential source or sink of carbon changes with time, season, and anthropogenic land use (Li et al., 2020; Wang et al., 2022, 2019). The carbon exchange over different ecosystems is primarily a function of the vegetation and the microclimate (Hu et al., 2024). For instance, in a non-water-limited grassland ecosystem,
60 the carbon fluxes are primarily controlled by soil temperature. In contrast, in a water limited ecosystem, the variation in carbon fluxes is primarily controlled by root-zone soil moisture (Wang et al., 2022).

Significant progress has been made in understanding the spatial-temporal variations in carbon and energy fluxes (Lin et al., 2017; Wang et al., 2022, 2020, 2021; Wang and Ma, 2022; Zhang et al., 2018; Zheng et al., 2022). However, the discrepancies between in-situ observations and more coarse scale modelling results need more
65 exploration. Zhao and Liu (2014), used the General Ensemble biogeochemical Modeling System (GEMS) to better understand the scale dependence of the simulated regional carbon balance in the South Eastern US. The study focused on the impacts of spatial resolution of the input data on the regional carbon dynamics, but the scope of the study did not aim to see how fluxes change with increasing spatial scales. In EC flux tower measurements, the observed area depends on the measurement height. The greater the height above the surface, the larger the spatial
70 scale. However, only a few studies investigated the changes in carbon fluxes at various heights over ecosystems with varying degrees of heterogeneity (Klosterhalfen et al., 2023; Krasnova et al., 2022). CO₂ fluxes (NEE) were investigated at a height of 30 m and 70 m over a heterogeneous mixed hemiboreal forest at the Järvselja Experimental Forestry Centre (Krasnova et al., 2022). The yearly accumulated carbon budget from the 30 m EC ($359 \pm 130 \text{ g C m}^{-2} \text{ y}^{-1}$) was different from the 70 m EC unit ($-46 \pm 120 \text{ g C m}^{-2} \text{ y}^{-1}$). The 70 m estimates reflected



75 a yearly budget comparable to other forest ecosystems, showing better mixing and natural integration of CO₂
fluxes further above the surface. On the contrary, the 30 m system detected local heterogeneities that affected the
annual CO₂ budget. Klosterhalfen et al. (2023) compared single-level EC measurements with two-level
concurrent EC measurements (60 m and 85 m) to investigate the impact of source area heterogeneity on flux
80 estimates over a managed boreal forest landscape. The study quantified the bias in the fluxes (GPP, Reco, H, LE,
and NEE), but was confined to discussing the limitation of using single-level flux estimates for model-data fusion
studies, site comparisons, and up- or downscaling of land-atmosphere exchange processes.

Unlike a mixed, disturbed landscape (Krasnova et al., 2022), the TP alpine steppe presents a relatively undisturbed,
rather homogeneous ecosystem allowing the study of complex interactions at varying spatial scales. Nieberding
et al., (2020, 2021) studied in-situ CO₂ fluxes from the alpine steppe ecosystem at Nam Co, spanning 14 years of
85 flux observations along with meteorological variables and plant cover estimations. The authors revealed a long-
term increase in CO₂ uptake, mainly caused by increased atmospheric temperatures during winter and a shift in
summer monsoon precipitation. Extending this research, the net ecosystem exchange (NEE) of CO₂ was estimated
at a measurement height of 19 m and compared with the long-term flux observation measured at a height of 3 m
at the same site. The source area of the 3 m measurements is relatively homogenous, and exhibits minimal
90 variation in vegetation types and density, making it a suitable reference for understanding the baseline patterns in
the fluxes. In contrast, the source area of the 19 m measurement covers a larger area that includes steppe vegetation
with small variations in vegetation density and a portion of the adjoining lake. The variation in the vegetation
density and the presence of the lake in the 19 m source area are integral to understand how these spatial
components in the footprint affect the overall carbon dynamics within the alpine steppe ecosystem. We
95 hypothesize that the chosen spatial scale will have a significant influence on what flux magnitude can be
considered representative for the area, with the flux determined by the vegetation distribution, soil properties (over
the dry steppe and the wet neighbouring land cover), the neighbouring lake, and the wind dynamics (Biermann et
al., 2014). By evaluating the variations in carbon fluxes with changes in sensor height, the present study
emphasizes the importance of shifting the focus from ecosystem-specific to landscape-level analyses. A
100 landscape-scale perspective captures the interactions between diverse ecosystems and their combined influence
on carbon fluxes, enabling more comprehensive and accurate upscaling approaches. Also, the results of this study
will help in identifying the optimal spatial scales for representing flux heterogeneity in high-altitude regions.

This study primarily aims to explore the variations in carbon fluxes across different spatial scales by examining
the fluxes at two sensor heights. While it provides an initial overview of flux variability within the study area, a
105 more detailed examination of the underlying drivers (e.g., vegetation structure, soil properties, or microclimate)
will be the focus of future research. The current analysis serves as a foundation for understanding flux variability,
with plans for subsequent studies to investigate the specific factors that contribute to these variations.

2 Methods

2.1 Study site

110 Nam Co Station for Multi-sphere Observation and Research (NAMORS) is located about 220 km north of the
Tibetan capital Lhasa, on the southeast shore of the Nam Co Lake (30°46' N, 90°57' E, 4730m a.s.l.). Strong
seasonality with long, cold winters and short but moist summers is the characteristic climate prevailing in the Nam
Co region. The mean daily temperature ranged between -22 °C to 14 °C during the period 2006 to 2017. The mean



115 annual temperature observed according to the data from 2006 to 2017 was mostly below zero and ranged from -
1.6 °C to 0 °C. The monthly mean temperature remained above zero in May, June, July, August, and September
in all the years. The majority of the precipitation was observed from May to October (Anslan et al., 2020) with
peaks either in August, July, or September. The mean annual precipitation is 405.6 mm, with the minimum and
maximum precipitation ranging from 291.1 mm (2015) and 568.8 mm (2010) respectively. The soil in the regions
is typical alpine steppe soil with very low clay content (Zhu et al., 2015) sustaining a mixed steppe vegetation
with C3 species like *Stipa purpurea* and *Kobresia pygmaea* with a very low plant height of 1 to 10 cm. The
growing season mostly starts at the end of April or the beginning of May and extends till September with
maximum biomass in late July or August. The annual mean soil temperature in the study area is found to be around
9.0 °C and the mean daily soil temperature varied from -20.1 °C to 34.8°C. The mean soil moisture observed was
low and reaching up to 29 % during the period 2006 to 2017.

125

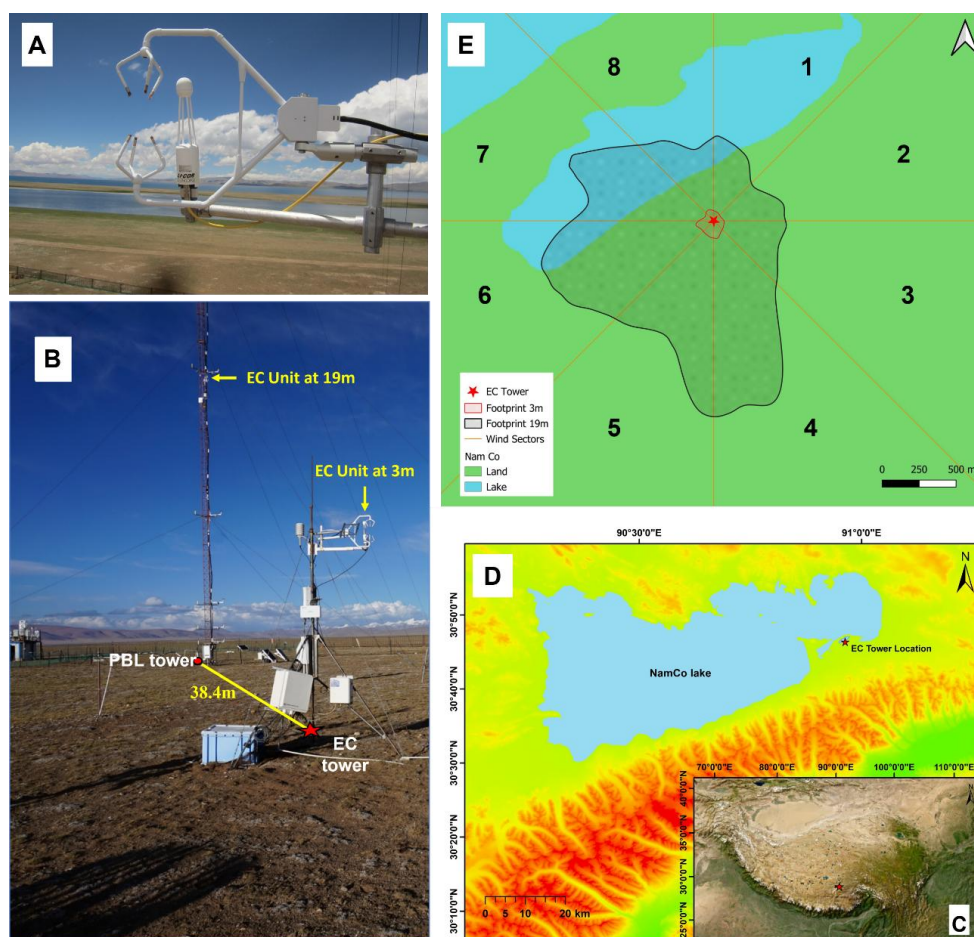


Figure 1. The 19m EC unit (Photo credit: Felix Nieberding) (A), the EC set up at the station (B, photo by Felix Nieberding), © Google Earth imagery showing the location of the Nam Co station on the TP (C), the



study area at the NAMORS station -SRTM DEM (D), the 90 % footprint climatology for the 3 m (red) and 19 m (black) EC measurement heights along with wind sectors (angular range of 45°) numbered 1 to 8 (E)

- 130 The micro-meteorological station consists of a 52 m tall planetary boundary layer (PBL) tower and a 3m eddy covariance measurement tower equipped with a CSAT3 ultrasonic anemometer (USA) and an LI-7500 open-path infrared gas analyzer (IRGA). The site was established in September 2005 by the Institute of Tibetan Plateau Research (ITP), Chinese Academy of Sciences (CAS) (Ma et al., 2009; Nieberding et al., 2020; Zhu et al., 2015). The station is equipped with instruments measuring air temperature (T_{air}) and relative humidity (RH) at five
- 135 different levels (1.5, 2, 4, 10, 20 m), wind speed and wind direction at three different levels (1.5, 10, 20m), soil moisture (SMC) and soil temperature (T_{soil}) at six different depths (0, 10, 20, 40, 80, 160 cm), soil heat flux at two different depths (10, 20 cm), radiation (short and long wave at 1.5m), air pressure, precipitation (PPTN), and a photosynthetic photon flux density sensor (PPFD- from 2013). For detailed information on instruments, see (Ma et al., 2009)
- 140 To evaluate the fluxes as a function of spatial scale, an additional measurement unit with CSAT3 ultrasonic anemometer and Li-7500RS open-path infrared gas analyzer was installed at a height of 19 m on the PBL tower from July 2018 onwards. The horizontal distance between the EC tower (ECNM-3m) and the PBL tower (ECPBL-19 m) is 38 m (Figure 1).

2.2 Data Processing

145 2.2.1 EC raw data processing at 19m height

- The EC method quantifies the CO_2 exchange between the surface and the overlying atmosphere by measuring the covariance between fluctuations in vertical wind velocity and CO_2 mixing ratio (Baldocchi, 2003). The 10 Hz one-year data acquired at the Nam Co site at a height of 19 m were used to calculate the 30-minute averaged fluxes of CO_2 (NEE), water vapor (H_2O), sensible heat (H), and latent heat (LE) using the raw data processing
- 150 software EddyPro (v7.0.9, LI-COR Inc.). The dataset analyzed in this study spans from 01 August 2018 to 31 May 2019. The standard EC correction procedures like despiking, coordinate rotation, detrending, lag time correction, frequency response corrections/spectral corrections, SND correction, and Webb-Pearman-Leuning (WPL) corrections were applied consistently with the procedure applied for the 3-m dataset by Nieberding et al. (2020). The data quality flagging policy according to Mauder and Foken (2006) was used to filter out best-quality
- 155 fluxes. The combined flag attains the values 0, 1, and 2. The value “0” for best quality fluxes, “1” for fluxes suitable for general analysis such as annual budgets, and “2” for fluxes that should be discarded from the results dataset. Only records with quality flags 0, and 1 were used and those with quality flag 2 were removed. The data were also subjected to statistical outlier removal. The data points that fell outside three standard deviations from the daily mean were eliminated. The data gaps in the flux measurements after all quality controls were filled using
- 160 the REddyProc R package (Wutzler et al., 2018) to apply the marginal distribution sampling (MDS) gap-filling algorithms, which is a moving window average method where both fluxes and the driving environmental variables are used for gap filling (Reichstein et al., 2005). The half-hourly NEE values were partitioned into gross primary productivity (GPP) and ecosystem respiration (R_{eco}) using Lasslop et al., (2010). The fluxes were grouped into different time scales (daily, and monthly) for the analysis.



165 **2.2.2 EC data at 3m height**

The current study used the fully processed and quality-controlled EC flux data set from the 3m EC tower at Nam Co from one of the authors of this manuscript (Nieberding et al., 2020). The 10 Hz EC raw data collected for the period from 2006 to 2019 from the small EC tower at 3m height were processed to 30 min averaged fluxes of CO₂, water vapor (H₂O), sensible (H), and latent heat flux (LE) in the raw data processing software EddyPro (v7.0.4, LI-COR Inc.). Drift correction, quality filtering, and sensor self-heating correction were applied to the data. The fluxes originating from possibly disturbed wind sectors were excluded. The CO₂ flux gaps were filled using the MDS gap fill algorithm in the REddyProc R package (Wutzler et al., 2018) and used for further analysis. For more details, see (Nieberding et al., 2020).

Large data gaps existed in the years 2012 to 2015 and 2018 to 2019. We ensured that the processing scheme applied to both datasets was identical to allow a robust and meaningful comparison between the two different measurement heights. The growing and non-growing seasons in the current study were defined based on the literature (Yun et al., 2022). For the current study, the months of May, August, and September were included in the growing season and the months from October to April were included in the non-growing season. The detailed investigation of the spatial heterogeneity in fluxes was constrained by the data coverage during the 2018-2019 observation period. Due to instrument failure, the data overlap between the 3 m EC unit and the 19 m EC unit was restricted to the early growing season of 2019, specifically, from May 13 to June 3, 2019.

2.2.3 Footprint analysis

The relative contribution from each element of the surface area source/sink to the measured vertical flux or concentration at a specific point in time, for specific atmospheric conditions and surface characteristics is termed as 'flux footprint' (Kljun et al., 2015; Vesala et al., 2008). The measurement height, along with surface roughness and wind direction determines the dimension of the area contributing to a given flux measurement. Above a homogenous surface and under turbulent mixing conditions, the fluxes from all parts of the surface contribute equally to the flux strength, hence the height of a sensor should not influence the measurements. The height of the sensor matters on an inhomogeneous surface because, the measured signal depends on the part of the surface that has the strongest influence on the sensor (Schmid, 2002).

The major approaches used in footprint modelling include analytical models, Lagrangian stochastic particle dispersion model (LPDM), large eddy simulations (LES), and closure models (Vesala et al., 2008). The current study used the Kormann and Meixner (KM) footprint model (more details in (Kormann and Meixner, 2001)) to analyze the influence of the source area in the measures fluxes. The KM model is based on a modification of the analytical solution of the advection-diffusion equation for power law profiles of the mean wind velocity and eddy diffusivity. The model uses parameters like EC measurement height (z_m) in meter (m), roughness length (z_0) in m, mean wind speed (WS) in ms^{-1} , Monin-Obukhov length (L) in m, the standard deviation of crosswinds (sv) in ms^{-1} , friction velocity (u_{star}) in ms^{-1} , and wind direction (WD) in degrees.

2.2.4 Remote sensing

Alpine ecosystems frequently experience snow cover in the non-growing season, which can significantly influence the carbon release and uptake in this environment. To have a better understanding of the snow cover period at the Nam Co site, three sets of data were used. The maximum snow cover data for the period 2005 to 2018 was downloaded from the National Tibetan Plateau/Third Pole Environment Data Center (Muhammad and Thapa,



2020). For the 2019 period, the MOD10A2 product for the TP region was downloaded from the Earthdata website
205 (Hall and Riggs, 2015). The snow parameters like snow cover, snow depth, and snow density at hourly, as well
as monthly time scale, were downloaded from the ECMWF 5th generation (ERA5) reanalysis data (C3S, 2018;
Copernicus Climate Change Service, 2019). The hourly data was linearly interpolated into half-hourly time steps
for further analysis.

Sentinel-2 Level-1C (L1C) MSI data for the 20th May 2019 was downloaded using the Google Earth engine. All
210 the bands were downloaded separately and stacked to form a single imagery. Band 8 (NIR) and band 4 (red) were
used to derive the normalized difference vegetation index (NDVI) for May 2019. A classified map separating land
and lake was created visually.

2.2.5 Statistical and Computational Methods

To quantify the overall uncertainty in carbon flux estimates, we applied error propagation principles, combining
215 uncertainties from both flux data processing and gap-filling procedures. This method allowed us to assess the
reliability of our carbon flux estimates and understand the potential range of errors associated with our
measurements.

In addition to addressing uncertainty, various statistical methods were employed in the study to analyze the data.
The Wilcoxon rank-sum test was used to analyze significant differences in NEE and meteorological variables
220 between the 3 m and 19 m footprints. For the overlapping period in May 2019, the Wilcoxon signed-rank test was
applied to account for paired observations. To evaluate relative discrepancies in the monthly NEE budget between
the two heights, we utilized the symmetrical percentage difference (SPD). Furthermore, mean absolute difference
(MAD) and root mean square error (RMSE) were calculated to quantify the magnitude of differences in fluxes
between measurement heights. Finally, random forest (RF) analysis (Tyrallis and Papacharalampous, 2017) was
225 used to evaluate the importance of meteorological variables in explaining variations in NEE and Reco.

To assess the influence of wind direction on the distribution and dispersion patterns within the study area, the
footprint was divided into eight wind sectors each covering an angular range of 45°. This segmentation allows for
an analysis that accounts for directional variations in the spatial variables. The sectors were numbered sequentially
from 1 to 8, starting from the north (0°), with subsequent sectors following in a clockwise direction (Figure 1 E).
230 Additionally, to evaluate the hypothesis on the effect of the chosen spatial scale and the land cover components
on the carbon sequestration, the relative contribution of each land cover type, derived from the footprint analysis
was used (Biermann et al., 2014). The NEE budget of the 19 m footprint area for each month was recalculated
for land-only and land-lake systems. Half-hourly fluxes with more than 99% contribution from land were
classified as land-exclusive fluxes (primarily from the wind sectors 2 to 5), while other fluxes included mixed
235 contributions from both land and lake. The monthly NEE budget for the land-lake system (wind sectors 6, 7, 8,
and 1) was obtained by subtracting the land-exclusive NEE budget from the total monthly NEE budget for the
entire footprint. For each month, the relative contribution of the land-lake system to the overall NEE was
calculated by taking the ratio of land-lake NEE to the total NEE. This provides insight into the role of land and
the land-lake system in overall carbon exchange. The calculated contributions were then analyzed to identify
240 monthly patterns and potential influencing factors. A key limitation of this approach is that the partitioning of
fluxes into land-exclusive and land-lake contributions was performed after gap-filling, rather than before. As a
result, the final datasets for each category (land vs. land-lake system) may have gaps that do not fully cover all



hours of the diurnal cycle, potentially introducing bias in the estimated monthly NEE budgets. Despite this limitation, the current method still provides a reasonable estimate of the relative contributions of land and land-lake systems to the overall NEE. Furthermore, the vegetation contribution to the NEE for 3 m and 19 m footprints was examined using the footprint-weighted NDVI. NDVI values were analyzed for each wind sector, as well as for the entire footprint area.

3 Results

3.1 Fluxes measured at 19 m

In this section, we present the observed carbon and energy fluxes measured at 19 m over the period 2018–2019. While values for each of the fluxes are provided, the subsequent sections will primarily focus on NEE, given its pivotal role in characterizing carbon exchange within this particular ecosystem. Continuous half-hourly flux data for the present analysis cover the period from 01st August 2018 to 31st May 2019 are provided. By convention, fluxes directed from the atmosphere to the surface have negative values and fluxes from the surface to the atmosphere have positive values. During the period, the alpine steppe at Nam Co acted as a sink of carbon in the growing season and as a source of carbon in the winter months. The source effect of the ecosystem prevailed long in the study period starting from October 2018 until the end of March 2019, making the system carbon neutral in the 10-month period. The daily mean NEE values ranged from -1.45 to 2.89 $\text{g C m}^{-2} \text{ day}^{-1}$, while the mean daily GPP ranged from -0.02 to -4.04 $\text{g C m}^{-2} \text{ day}^{-1}$. The mean Reco varied from 0.05 to 4.80 $\text{g C m}^{-2} \text{ day}^{-1}$. On a monthly scale, maximum net fixation occurred in May 2019 (-25.77 ± 4.7 $\text{g C m}^{-2} \text{ month}^{-1}$) followed by August 2018 (-24.67 ± 7 $\text{g C m}^{-2} \text{ month}^{-1}$) and the maximum release occurred in December 2018 (28.64 ± 4.7 $\text{g C m}^{-2} \text{ month}^{-1}$). The highest values of GPP were found in August (-76.93 ± 5.8 $\text{g C m}^{-2} \text{ month}^{-1}$) and September 2018 (-63.07 ± 7.7 $\text{g C m}^{-2} \text{ month}^{-1}$) and Reco in September (59.06 ± 5.4 $\text{g C m}^{-2} \text{ month}^{-1}$) and August 2018 (56.80 ± 5.3 $\text{g C m}^{-2} \text{ month}^{-1}$). The partitioned values of GPP in November and December were less than -6 $\text{g C m}^{-2} \text{ month}^{-1}$ with uncertainties of ± 3.3 and ± 6.2 $\text{g C m}^{-2} \text{ month}^{-1}$ respectively implying reduced photosynthesis by freezing air temperature and low radiation.

3.2 Meteorology

The air temperature and soil temperature varied from -21 °C to 11 °C and -11 °C to 17 °C, respectively. Negative air temperature was observed from October 2018 to mid-April 2019. Most of the precipitation occurred in August and September and minimal precipitation in May 2019. The soil moisture in the study area was comparatively low ranging from 4 to 26 %. The data for soil temperature, soil moisture, and precipitation, were missing in the winter months. The soil moisture correlated well with precipitation, except in April 2019, which showed comparatively higher soil moisture with less or no rainfall, probably caused by melting snow cover. The months that received maximum precipitation were August (123.8 mm), October (71.4 mm) and September (70.4 mm). The months of February, March, April, and May 2019 received 0.5, 2.1, 1.4, and 4.3 mm of precipitation respectively. The monthly soil temperature, air temperature, and soil moisture were highest in August 2018. The daily vapour pressure deficit varied from 0.585 to 7.632 hPa. The months of May 2019 (4.49 hPa), August 2018 (4.41 hPa), and September 2018 (4.42 hPa) showed less variation in the monthly VPD. Monthly VPD was least in January (1.31 hPa) and December (1.67 hPa). Maximum PAR was observed in May 2019 (1597 mol photons $\text{m}^{-2} \text{ month}^{-1}$), followed by April 2019 (1494 mol photons $\text{m}^{-2} \text{ month}^{-1}$), and the least in December 2018 (562 mol photons $\text{m}^{-2} \text{ month}^{-1}$). The daily radiation data was missing in January and February.



3.3 Comparison of the fluxes at 19m and 3m

The NEE budgets (Figures 2 and 3) in the study site measured at 19 m height were compared with the long-term values measured at 3 m height. The monthly NEE values diverged significantly between the 19 m and the 3 m measurement heights (Wilcoxon rank sum test, $p < 0.001$) during the winter months (November to March) and in May. The 3 m source area predominantly acted as a sink throughout most months across all years. However, it occasionally acted as a slight carbon source in November, December, January, and October in specific years. For instance, positive NEE (indicating net source behaviour) was observed at 3 m footprint in the years 2007 to 2009 in October; 2006 to 2009 and 2017 in November; 2006 to 2008 in December; 2006, 2008 and 2009 in January. The symmetrical percentage difference (SPD) analysis further underscored the deviations in the monthly NEE budget between 19 m and 3 m measurement heights. The extreme negative SPD values (-200 %) in October, December, February and March indicate that the carbon sink strength at 19 m was substantially lower compared to 3 m during these months. Similarly, November and January showed significant reductions in carbon sink strength at 19 m, with SPD values of -159.3% and -198.7%, respectively. Conversely, the low SPD values closer to zero in August, September, April or positive SPD values (+ 55.9 %) in May indicated comparable to or even greater carbon sink strength at 19 m footprint than 3 m footprint.

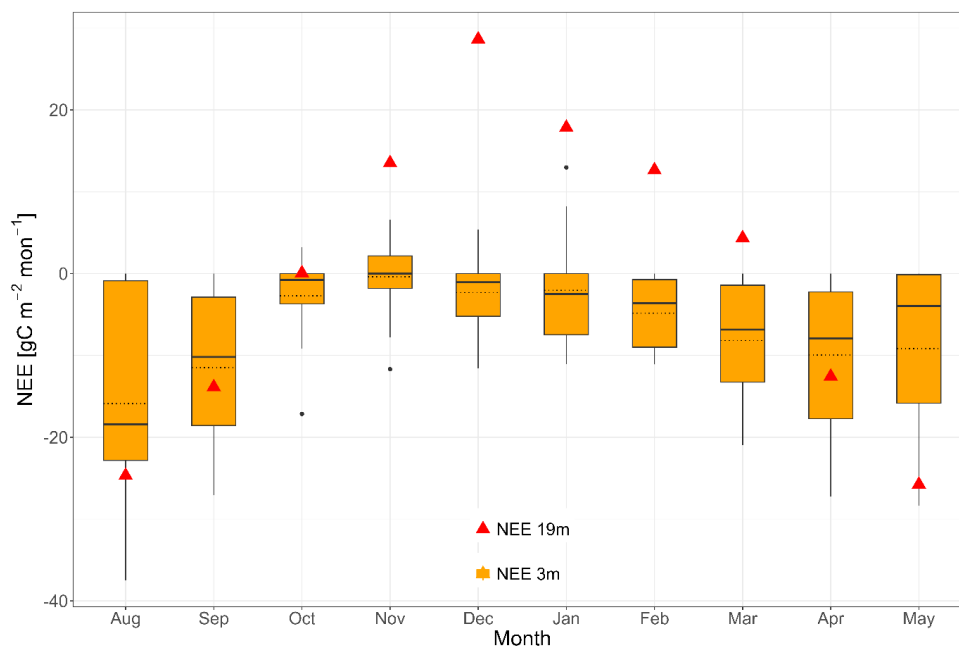


Figure 2. Comparison of monthly NEE budget at Nam Co (alpine steppe ecosystem) for two different EC measurement heights. The boxplot in the figure represents the distribution of the monthly NEE budget over the period from 2006-2007 to 2016-2017 (major gaps in 2012--2016) observed at 3 m and the red symbols represent the monthly NEE budget observed during August 2018- May 2019 measured at 19 m. The dark line represents the median and dotted one the mean.



The ten-month cumulative NEE budget (August of the current year to May of the consecutive year) estimated at Nam Co for the 3 m footprint area ranged from $-154.6 \pm 14 \text{ gC m}^{-2}$ to $-22.2 \pm 9.4 \text{ gC m}^{-2}$ with a mean of $-78 \pm 11.3 \text{ gC m}^{-2}$ for the ten month period implying that the ecosystem acted as a consistent sink of carbon from 2006-2007 to 2017-2018. The 2010-2011 and 2016-2017 were the periods with the highest net fixation for the 3 m height. The periods from 2011-2012 to 2015-2016, and 2017-2018 had larger data gaps and were not used for the carbon budget quantification. On the other hand, we estimated a NEE of $0.229 \pm 15.2 \text{ gC m}^{-2}$ at the 19 m EC-system during the 2018-2019 period, indicating that the ecosystem acted approximately carbon neutral. To see the temporal variability in the seasonal distribution of the carbon budget, the growing season (GS) and non-growing season (NGS) carbon fluxes were also analyzed. The seasonal analysis showed a significant difference (Wilcoxon rank sum test, $p < 0.001$) in the NEE over the 19 m footprint from the long-term NEE observed on the 3 m footprint in the non-growing season (NGS), reaffirming the key importance of the NGS carbon fluxes in regulation of the annual carbon budget of an alpine ecosystem. Ecosystem respiration in the non-growing season accounted for about 35% of the total ecosystem respiration at the 3 m and 57 % of the total ecosystem respiration at the 19 m.

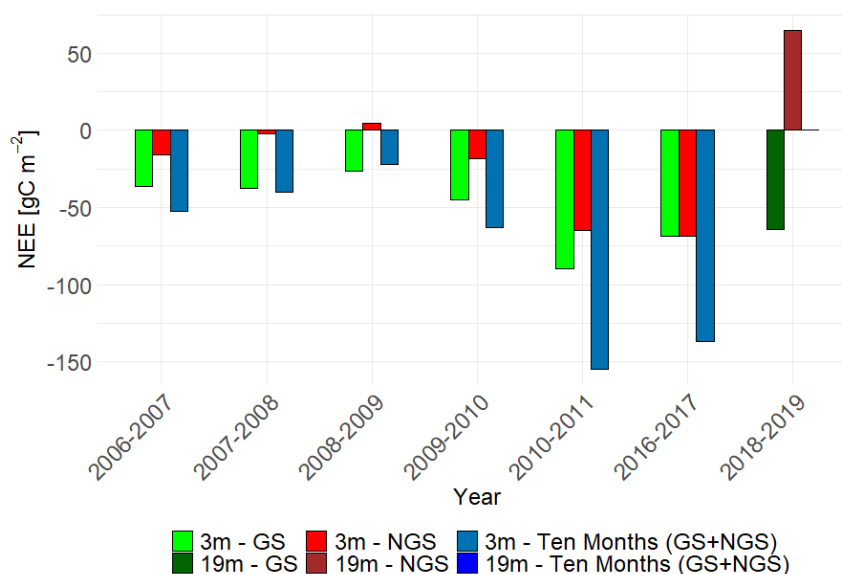


Figure 3. NEE budget at Nam Co split into growing season (GS), non-growing season (NGS) & 10-month integrated. The period 2018-2019 shows the NEE budget at 19 m and other periods in the x-axis show the NEE budget at 3 m.

3.4 Snow cover pattern

Nam Co experienced different amounts of snow cover in each period from 2006-2007 to 2018-2019 (Figure 4). The snow parameters like snow density, and snow depth observed in 2018-2019 were significantly different (Wilcoxon rank sum test, $p < 0.001$) from the other periods. The monthly snow depth in the winter months of the 2018-2019 period varied between 13 cm (October) to 33 cm (January) with an average snow depth of 26 cm. The winters 2006-2007, 2008-2009, and 2014-2015 also had considerable snow cover in Nam Co. The average snow depth for the period 2006-2007 and 2008-2009 were found to be 20 cm, and 8cm respectively. The year 2014-



2015 had a greater number of snow-covered days, but the snow depth was minimal (1 cm). The years 2007-2008 and 2010-2011 had the same number of snow-covered days, but the snow depth in 2010-2011 was slightly more than in 2007-2008. Although a few studies found significant relationships between snow cover and vegetation activity at higher altitudes (3500-4200m), the impact of snow cover in controlling the fluxes (carbon and energy) is not completely understood (Qi et al., 2021).

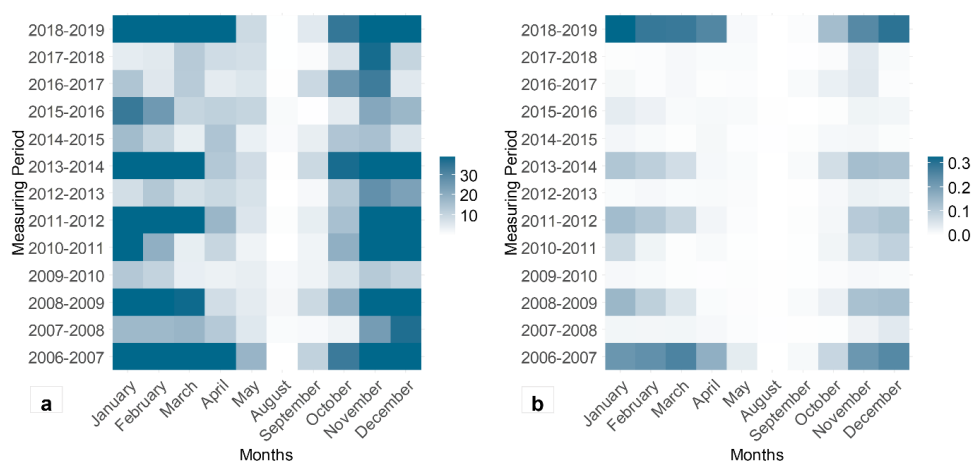


Figure 4. a) Monthly snow cover (%) and b) snow depth (m) at NAMORS

3.5 Spatial influences on fluxes measured at 19m and 3m

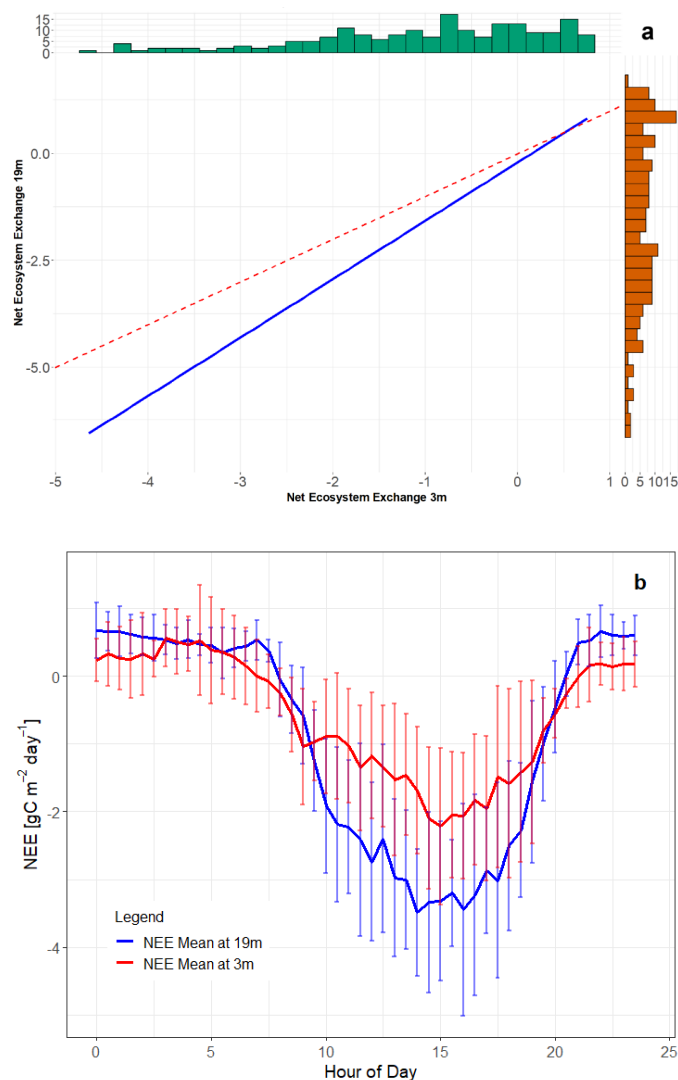
To understand the influence of the lake on the NEE budget measured at the 19 m system, the NEE budget was calculated separately for the whole system (0.23 g C m^{-2}) and land alone (56 g C m^{-2}). These results indicate that the land-lake system (south-west to north-east direction) plays a significant role in carbon sequestration by masking emissions from the land (north-east to south west direction). Specifically, the land-lake system's relative contribution led to enhanced net carbon uptake in August (40%), September (108%), April (92%), and May (55%). Conversely, in October, November, January, and March, the land-lake system reduced net emissions by offsetting those from the land. In December, both the land and the land-lake system contributed positively to carbon emissions.

Due to instrument failure, the data overlap between the 3 m EC unit and the 19 m EC unit was limited to the early growing season 2019. The data from May 2019 were analyzed for the diurnal trend and differences between the two measurement heights. All half-hourly fluxes estimated at 3 m at NAMORS were positively correlated with the fluxes estimated at 19 m (Figure 5a). The high correlation for the NEE (0.85) indicates a similar temporal dynamic but difference in the magnitude of the fluxes can be observed. The examination of the mean diurnal cycle of NEE during the period implies slightly more night-time respiration and substantially more mid-day net carbon uptake in the 19 m EC system than in the 3 m EC system (Figure 5b).

The fluxes originating exclusively from the land area during the overlapping period showed a statistically significant difference (Wilcoxon signed rank test, $p = 0.0013$) between the NEE measured at 3 m and 19 m. However, the magnitude of the difference measured using the rank biserial correlation (0.1) implied that the difference observed is of limited practical importance. Additionally, the Spearman correlation analysis revealed a



355 very strong positive monotonic relationship ($\rho = 0.94$), suggesting that despite the differences, the measurements generally trend together. To further evaluate the agreement, mean absolute difference (MAD) and root mean square error (RMSE) were calculated. The MAD and RMSE were found to be 0.827 and 1.02 $\text{g C m}^{-2} \text{ day}^{-1}$ respectively. The results indicate a proportional bias rather than a consistent bias in one direction. The differences were higher at higher negative NEE values, suggesting that the bias is not uniform but instead varies systematically with the magnitude of NEE.



360 **Figure 5. (a) Correlation between NEE estimated at 3m and 19m height at Nam Co Station; (b) Diurnal Cycle of NEE – Early Growing Period (May 2019). The red solid line represents the mean NEE measured at 3 m and blue solid dark line represents the mean NEE measured at 19 m. Error bars, represented by light vertical lines, indicate the standard deviation at each time point.**



3.6 Wind sector analysis

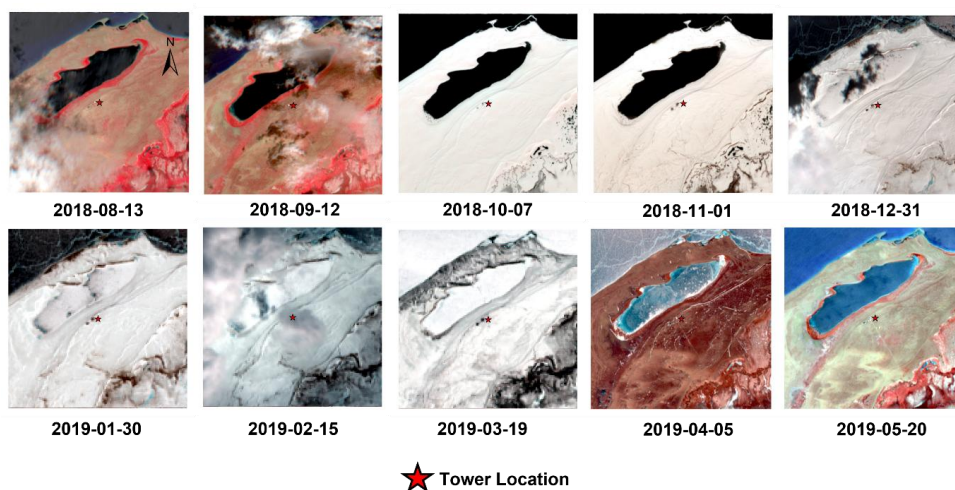
365 The mean NDVI values were found relatively similar or higher in 3 m as compared to 19 m, except in wind sectors
4 (135° - 180°, South-East to South) and 3 (90° - 135°, East to South-East). The standard deviation in the 19 m
footprint for all the wind sectors was higher. The maximum standard deviation of NDVI was found in the wind
sector 8 (315° to 360°, North-West to North), and 7 (270° to 315°, West to North-West). The deviation of NDVI
was found similar in the wind sector 5 (180° to 225°, South to South-West). The wind sector analysis partitioned
370 for day and night in May revealed that the highest contribution of fluxes (78 %) in the daytime was obtained from
the north-westerly wind sectors (6, 7, 8, 1) and 12 % from the South-East to South (wind sector 4). In the night-
time, 59 % of the total contribution was from the south-westerly sectors 4 (37 %), 5 (12 %), 3 (10 %), and 36 %
from the north-westerly wind sectors. It means, that during the day, the higher uptake shown by the 19 m footprint
was mostly contributed by the land-water continuum, whereas at night, the higher respiration shown by the 19 m
375 footprint was mostly contributed by the land.

4 Discussion

Carbon and energy fluxes over the region are mostly driven by local meteorology and the spatial composition of
the landscape. By increasing the measurement height from 3 m to 19 m, the present study explores the variability
in the estimated fluxes in both space and time. The long-term estimate based on the 3 m data for the ten-month
380 period agreed with the average yearly NEE estimate of the alpine steppe ($-64.3 \pm 38.7 \text{ g C m}^{-2} \text{ yr}^{-1}$) and the alpine
meadow steppe ($-66.7 \text{ g C m}^{-2} \text{ yr}^{-1}$) ecosystem of the TP (Li et al., 2021; Wei et al., 2021). Nieberding et al. (2021)
reported the alpine steppe at Nam Co as a carbon sink with a widespread greening at the southern shore of Lake
Nam Co. The modified Mann-Kendall trend tests based on the 14 years of carbon flux and meteorological data
(2006-2019) measured at 3 m height showed an increase in the daily NEE at a rate of $0.5 \text{ g C m}^{-2} \text{ decade}^{-1}$,
385 depicting more carbon storage than release. In the current study, we found slightly more CO₂ release than uptake
when increasing the measurement height to 19 m (2018-2019) and thus enlarging the footprint. The monthly scale
NEE budget showed a more significant difference in the winter months. The percent contribution of the winter
respiration of the larger footprint was in agreement with the result reported for the alpine steppe near the Beilu'He
research station, a continuous permafrost area of the northern Qinghai-Tibetan Plateau (Yun et al., 2022). The
390 authors found that 51% of the annual ecosystem respiration of the alpine steppe near Beilu'He research station
was accounted for by the winter respiration. The months from October to March showed a continuous net release
of carbon, which coincided with the period with negative air temperature, low solar radiation, and prolonged snow
cover (Figure 6). The variable snow depth affects carbon cycling in winter (Wang et al., 2020), while
micrometeorology and vegetation activity in the snow-free periods influences the size and variability of the winter
395 fluxes (Merbold et al., 2012). Winter snow cover is beneficial for vegetation since it reduces root mortality from
the freezing temperatures. At the same time, longer snow cover can reduce the GPP by delaying the begin of the
vegetation period (Liu et al., 2023). The spatial distribution of snow directly controls soil temperature and
indirectly the vegetation and the quality of organic matter. The snow duration, snow cover, and snow depth affect
the CO₂ release (Bosiö et al., 2014; Liu et al., 2023). Using RF, the different meteorological parameters tested
400 against NEE and Reco in winter revealed a high dependency (49 %) of Reco on snow depth. This implies that one
of the major causes of the significant difference in emissions observed by the 19 m measurements during winter



could be the extreme snow cover during the 2018-2019 period. Another probable cause might be the spatial heterogeneity introduced by the larger footprint.



405

Figure 6. Satellite Imagery (FCC) – Nam Co – 2018 & 2019

The simultaneous measurements taken at 19 m and 3 m heights supported the influence of spatial heterogeneity on the observed flux measurements in the steppe. The higher rates of carbon uptake and release observed at 19 m suggest that the larger footprint encompasses more diverse micro-environments which respond differently to meteorological conditions than the more localized measurements at 3 m. The NDVI values within the 90% footprint area highlighted notable differences in spatial heterogeneity between the 3 m and 19 m footprints. Specifically, the broader NDVI range in the larger 19 m footprint (-0.14 to 0.34) indicates the presence of both vegetation and water bodies. In contrast, the more constrained NDVI range in the 3 m footprint (0.09 to 0.19) implies a more homogeneous land cover predominantly composed of vegetation and patches of bare soil. The preliminary analysis of footprint-weighted NDVI values (excluding the lake area) showed that mean vegetational contributions were similar between the two footprints (0.11 for 3 m and 0.10 for 19 m), challenging the initial hypothesis that higher CO₂ uptake in the larger footprint was a result of increased vegetation cover. This finding implies that other factors, such as the spatial distribution of land cover types and the presence of water bodies, may be influencing flux measurements at 19 m. Li et al. (2024) quantified the flux strength from the small lake, finding it to act as a CO₂ sink during May. Additionally, the footprint-weighted land cover analysis in May revealed that the 19 m footprint contained a mix of land and lake contributions, with the half-hourly contribution from water reaching up to 71 % of the total contribution, whereas the 3 m flux contribution was almost exclusively from the mainland (98%).

The decomposition of fluxes based on the relative contributions of land and land-lake system highlights the varying roles these systems play in the overall carbon dynamics of the larger footprint. The cooler water temperature in lakes enhances CO₂ solubility, thus more absorption of carbon. The higher lake contribution in April and October emphasizes their ability to enhance and counterbalance the land-derived carbon fluxes during



the transitional months. During May, as the land photosynthesis increases, the whole system exhibits a much stronger carbon sink ($-25.76 \text{ g C m}^{-2}$). The dropping of the relative contribution of the land-lake system to
430 54.81 % in May indicates that the land and lake dynamics are more balanced as temperatures rise and vegetation becomes more active. The results reveal that both land and lake exhibit strong seasonal variations. The lakes offset carbon emissions during periods of reduced land activity, while land assumes a larger role in carbon sequestration during peak vegetation growth. This results corroborate those of Premke et al. (2016), and highlights the need for understanding the integrated land-lake carbon dynamics, especially in regions where lakes play a significant role
435 in the ecosystem's carbon balance.

The fluxes primarily originating from land over the two footprints supported the footprint-weighted NDVI analysis, which indicated similar vegetation contributions between the footprints. Fluxes measured from land-dominated areas at both heights were largely comparable, highlighting the consistency of steppe-derived fluxes across measurement scales. The NEE budget for May, calculated based on land fluxes, was $-12.6 \pm 3.7 \text{ g C m}^{-2}$
440 and $-11.6 \pm 3.3 \text{ g C m}^{-2}$ for the 3 m and 19 m footprints, respectively. The MAD value suggests that the 3 m and 19 m measurements captured the same underlying process. However, the higher RMSE compared to MAD indicates the presence of some substantial discrepancies, likely arising from areas within the 19 m footprint exhibiting either elevated or reduced carbon fixation rates relative to the 3 m footprint. Given the inherent variability that exists across different spatial scales, the observed difference may be reasonable. However, it's
445 important to note that the data solely originating from land represents only 25% of the total overlapping dataset in May. Large discrepancies, particularly those highlighted by RMSE, warrant further investigation to determine whether they are linked to specific times, environmental conditions, or spatial features.

A key limitation of this study is the short overlapping period between the two measurement heights. While fluxes at 19 m were measured from August 2018 to May 2019, the long-term 3 m flux dataset spans 2006 to 2019, with
450 only three weeks of direct overlap in May 2019. This limited overlap restricts our ability to draw definitive conclusions about carbon flux variations across different spatial scales. Despite this, the study aimed to explain spatial variability using the 10-month dataset from the 19 m height, which represents a larger footprint area. Although this provides a broader spatial perspective, the comparison with long-term 3 m data introduces potential uncertainties related to interannual variability, as flux differences may be influenced by environmental changes
455 across years rather than solely by spatial scale. Another limitation is the uncertainty associated with the data from the land-lake system. The inherent variability and potential noise in carbon flux measurements may hinder the quality of the decomposition of carbon fluxes into contributions from land and lake components. Due to this, we did not perform a detailed decomposition of fluxes into land and lake contributions, which hinders our ability to accurately assess their individual impacts on overall carbon dynamics. Future studies should aim to address these
460 uncertainties and refine the separation of flux contributions for a clearer understanding of the land-lake system dynamics.

These results support the hypothesis that spatial scale significantly impacts flux estimates, particularly in heterogeneous alpine landscapes where vegetation distribution, soil properties, neighbouring lakes, and wind dynamics play critical roles. By highlighting the impact of spatial scale on flux representation in such landscapes,
465 this study underscores the importance of considering landscape-level variability when interpreting flux measurements. These insights are crucial for developing more reliable gridded surface flux maps, thereby reducing



carbon budget discrepancies. Future research, with longer concurrent measurement at multiple heights, will focus on disentangling the underlying drivers, such as vegetation structure, soil properties, and microclimate, to build on this foundational understanding and advance landscape-scale carbon flux modelling.

470 5 Conclusion

This study contributes to the growing body of literature on carbon fluxes by using a dual-tower approach to investigate the dynamics of carbon release and sequestration in an alpine landscape. Notably, we observed the sensor at 19 m height recorded higher absolute net ecosystem exchange (NEE) values. This discrepancy was particularly pronounced during non-growing periods, driven by the extreme snow event during winter 2018-2019, which emphasizes the critical role of seasonal dynamics and environmental conditions in shaping carbon dynamics. The influence of the neighboring lake on carbon dynamics over larger footprints was substantial, with lake-land interactions contributing considerably to the observed fluxes. The land-based fluxes measured at 3 m height, aligned closely with the fluxes reported for other steppe ecosystems in TP, suggesting the 3 m measurements represent the terrestrial contributions, but may fail to capture the broader landscape-level heterogeneity.

Our findings support the hypothesis that spatial scale strongly influences carbon flux measurements, with larger-scale assessments better capturing integrated effects of diverse ecosystems such as steppe and adjacent lakes. These results emphasize the need to integrate aquatic and terrestrial fluxes into upscaling models to improve the accuracy of carbon budget estimates. Overall, this study highlights the necessity of adopting a landscape-scale perspective to account for flux variability across heterogeneous environments. Such an approach is crucial for developing more reliable gridded surface flux maps, reducing uncertainties in carbon budgets, and improving predictions of ecosystem responses to environmental change. These insights could also enhance our understanding of localized emission patterns and support more informed environmental management practices.

Data availability

490 The dataset will be made available upon request to the corresponding authors.

Author Contributions

NP, CW, MH, and TS conceptualized the study. NP and CW processed raw data and did the quality control. FN contributed to instrumentation, data acquisition and long-term data curation. TS conceived the project, acquired funding, and supervised the project. NP carried out the investigation, formal analysis, visualization and preparation of the original draft. All authors contributed to the reviewing and editing the original draft.

Competing interest

All the authors declare no conflict of interest for this work.

Acknowledgment

500 N.P. was supported by the DAAD Graduate School Scholarship Programme (GSSP). This research is a contribution to the International Research Training Group “Geoecosystems in transition on the Tibetan Plateau (TransTiP),” funded by the Deutsche Forschungsgemeinschaft (DFG) (grant no. 317513741/GRK 2309). We thank Yaoming Ma for supporting field work logistics and permitting and for the opportunity to mount additional sensors on the PBL tower.



505 **References**

- Anslan, S., Azizi Rad, M., Buckel, J., Echeverria Galindo, P., Kai, J., Kang, W., Keys, L., Maurischat, P., Nieberding, F., Reinosch, E., Tang, H., Tran, T. V., Wang, Y., and Schwalb, A.: Reviews and syntheses: How do abiotic and biotic processes respond to climatic variations in the Nam Co catchment (Tibetan Plateau)?, *Biogeosciences*, 17, 1261–1279, <https://doi.org/10.5194/bg-17-1261-2020>, 2020.
- 510 Baldocchi, D. D.: Assessing the eddy covariance technique for evaluating carbon dioxide exchange rates of ecosystems: past, present and future, *Global Change Biology*, 9, 479–492, <https://doi.org/10.1046/j.1365-2486.2003.00629.x>, 2003.
- Biermann, T., Babel, W., Ma, W., Chen, X., Thiem, E., Ma, Y., and Foken, T.: Turbulent flux observations and modelling over a shallow lake and a wet grassland in the Nam Co basin, Tibetan Plateau, *Theor Appl Climatol*, 116, 301–316, <https://doi.org/10.1007/s00704-013-0953-6>, 2014.
- 515 Bosiö, J., Stiegler, C., Johansson, M., Mbufong, H. N., and Christensen, T. R.: Increased photosynthesis compensates for shorter growing season in subarctic tundra—8 years of snow accumulation manipulations, *Climatic Change*, 127, 321–334, <https://doi.org/10.1007/s10584-014-1247-4>, 2014.
- C3S: ERA5 hourly data on single levels from 1940 to present, <https://doi.org/10.24381/CDS.ADBB2D47>, 2018.
- 520 Copernicus Climate Change Service: ERA5-Land monthly averaged data from 1950 to present, <https://doi.org/10.24381/CDS.68D2BB30>, 2019.
- Gilmanov, T. G., Johnson, D. A., and Saliendra, N. Z.: Growing season CO₂ fluxes in a sagebrush-steppe ecosystem in Idaho: bowen ratio/energy balance measurements and modeling, *Basic and Applied Ecology*, 4, 167–183, <https://doi.org/10.1078/1439-1791-00144>, 2003.
- 525 Hall, D. K. and Riggs, G. A.: MODIS/Terra Snow Cover 8-Day L3 Global 500m SIN Grid, <https://doi.org/10.5067/MODIS/MOD10A2.006>, 2015.
- Hu, Z., Wang, G., Sun, X., Huang, K., Song, C., Li, Y., Sun, S., Sun, J., and Lin, S.: Energy partitioning and controlling factors of evapotranspiration in an alpine meadow in the permafrost region of the Qinghai-Tibet Plateau, *Journal of Plant Ecology*, 17, rtac002, <https://doi.org/10.1093/jpe/rtac002>, 2024.
- 530 Kljun, N., Calanca, P., Rotach, M. W., and Schmid, H. P.: A simple two-dimensional parameterisation for Flux Footprint Prediction (FFP), *Geosci. Model Dev.*, 8, 3695–3713, <https://doi.org/10.5194/gmd-8-3695-2015>, 2015.
- Klosterhalfen, A., Chi, J., Kljun, N., Lindroth, A., Laudon, H., Nilsson, M. B., and Peichl, M.: Two-level eddy covariance measurements reduce bias in land-atmosphere exchange estimates over a heterogeneous boreal forest landscape, *Agricultural and Forest Meteorology*, 339, 109523, <https://doi.org/10.1016/j.agrformet.2023.109523>, 2023.
- 535 Kormann, R. and Meixner, F. X.: An Analytical Footprint Model For Non-Neutral Stratification, *Boundary-Layer Meteorology*, 99, 207–224, <https://doi.org/10.1023/A:1018991015119>, 2001.
- Krasnova, A., Krasnov, D., Cordey, H. P. E., and Noe, S. M.: Eddy-covariance carbon fluxes of a heterogeneous forest: one tower - two heights, *Biogeochemistry: Air - Land Exchange*, <https://doi.org/10.5194/egusphere-2022-384>, 2022.
- 540 Lasslop, G., Reichstein, M., Papale, D., Richardson, A. D., Arneth, A., Barr, A., Stoy, P., and Wohlfahrt, G.: Separation of net ecosystem exchange into assimilation and respiration using a light response curve approach: critical issues and global evaluation, *Global Change Biology*, 16, 187–208, <https://doi.org/10.1111/j.1365-2486.2009.02041.x>, 2010.
- 545 Li, H., Wang, C., Zhang, F., He, Y., Shi, P., Guo, X., Wang, J., Zhang, L., Li, Y., Cao, G., and Zhou, H.: Atmospheric water vapor and soil moisture jointly determine the spatiotemporal variations of CO₂ fluxes and



evapotranspiration across the Qinghai-Tibetan Plateau grasslands, *Science of The Total Environment*, 791, 148379, <https://doi.org/10.1016/j.scitotenv.2021.148379>, 2021.

- 550 Li, J., Gong, J., Guldmann, J.-M., Li, S., and Zhu, J.: Carbon Dynamics in the Northeastern Qinghai-Tibetan Plateau from 1990 to 2030 Using Landsat Land Use/Cover Change Data, *Remote Sensing*, 12, 528, <https://doi.org/10.3390/rs12030528>, 2020.
- Li, W., Wang, B., and Ma, Y.: Quantifying the CO₂ sink intensity of large and small saline lakes on the Tibetan Plateau, *Science of The Total Environment*, 938, 173408, <https://doi.org/10.1016/j.scitotenv.2024.173408>, 2024.
- 555 Lin, X., Han, P., Zhang, W., and Wang, G.: Sensitivity of alpine grassland carbon balance to interannual variability in climate and atmospheric CO₂ on the Tibetan Plateau during the last century, *Global and Planetary Change*, 154, 23–32, <https://doi.org/10.1016/j.gloplacha.2017.05.008>, 2017.
- Liu, H., Xiao, P., Zhang, X., and Wu, Y.: Increased snow cover enhances gross primary productivity in cold and dry regions of the Tibetan Plateau, *Ecosphere*, 14, e4656, <https://doi.org/10.1002/ecs2.4656>, 2023.
- 560 Liu, Y., Zhang, X., Du, X., Du, Z., and Sun, M.: Alpine grassland greening on the Northern Tibetan Plateau driven by climate change and human activities considering extreme temperature and soil moisture, *Science of The Total Environment*, 916, 169995, <https://doi.org/10.1016/j.scitotenv.2024.169995>, 2024.
- Lu, X., Yan, Y., Sun, J., Zhang, X., Chen, Y., Wang, X., and Cheng, G.: Carbon, nitrogen, and phosphorus storage in alpine grassland ecosystems of Tibet: effects of grazing exclusion, *Ecology and Evolution*, 5, 4492–4504, <https://doi.org/10.1002/ece3.1732>, 2015.
- 565 Ma, Y., Wang, Y., Wu, R., Hu, Z., Yang, K., Li, M., Ma, W., Zhong, L., Sun, F., Chen, X., Zhu, Z., Wang, S., and Ishikawa, H.: Recent advances on the study of atmosphere-land interaction observations on the Tibetan Plateau, *Hydrol. Earth Syst. Sci.*, 13, 1103–1111, <https://doi.org/10.5194/hess-13-1103-2009>, 2009.
- Mauder, M. and Foken, T.: Impact of post-field data processing on eddy covariance flux estimates and energy balance closure, *metz*, 15, 597–609, <https://doi.org/10.1127/0941-2948/2006/0167>, 2006.
- 570 Meeran, K., Ingrisch, J., Reinthaler, D., Canarini, A., Müller, L., Pötsch, E. M., Richter, A., Wanek, W., and Bahn, M.: Warming and elevated CO₂ intensify drought and recovery responses of grassland carbon allocation to soil respiration, *Global Change Biology*, 27, 3230–3243, <https://doi.org/10.1111/gcb.15628>, 2021.
- 575 Merbold, L., Rogiers, N., and Eugster, W.: Winter CO₂ fluxes in a sub-alpine grassland in relation to snow cover, radiation and temperature, *Biogeochemistry*, 111, 287–302, <https://doi.org/10.1007/s10533-011-9647-2>, 2012.
- Muhammad, S. and Thapa, A.: An improved Terra-Aqua MODIS snow cover and Randolph Glacier Inventory 6.0 combined product (MOYDGL06*) for high-mountain Asia between 2002 and 2018, *Earth Syst. Sci. Data*, 12, 345–356, <https://doi.org/10.5194/essd-12-345-2020>, 2020.
- 580 Nieberding, F., Wille, C., Fratini, G., Asmussen, M. O., Wang, Y., Ma, Y., and Sachs, T.: A long-term (2005–2019) eddy covariance data set of CO₂ and H₂O fluxes from the Tibetan alpine steppe, *Earth Syst. Sci. Data*, 12, 2705–2724, <https://doi.org/10.5194/essd-12-2705-2020>, 2020.
- 585 Nieberding, F., Wille, C., Ma, Y., Wang, Y., Maurischat, P., Lehnert, L., and Sachs, T.: Winter Daytime Warming and Shift in Summer Monsoon Increase Plant Cover and Net CO₂ Uptake in a Central Tibetan Alpine Steppe Ecosystem, *JGR Biogeosciences*, 126, e2021JG006441, <https://doi.org/10.1029/2021JG006441>, 2021.
- Piao, S., Wang, X., Park, T., Chen, C., Lian, X., He, Y., Bjerke, J. W., Chen, A., Ciais, P., Tømmervik, H., Nemani, R. R., and Myneni, R. B.: Characteristics, drivers and feedbacks of global greening, *Nat Rev Earth Environ*, 1, 14–27, <https://doi.org/10.1038/s43017-019-0001-x>, 2019.
- 590 Premke, K., Attermeyer, K., Augustin, J., Cabezas, A., Casper, P., Deumlich, D., Gelbrecht, J., Gerke, H. H., Gessler, A., Grossart, H., Hilt, S., Hupfer, M., Kalettka, T., Kayler, Z., Lischeid, G., Sommer, M., and Zak, D.:



The importance of landscape diversity for carbon fluxes at the landscape level: small-scale heterogeneity matters, *WIREs Water*, 3, 601–617, <https://doi.org/10.1002/wat2.1147>, 2016.

- 595 Qi, Y., Wang, H., Ma, X., Zhang, J., and Yang, R.: Relationship between vegetation phenology and snow cover changes during 2001–2018 in the Qilian Mountains, *Ecological Indicators*, 133, 108351, <https://doi.org/10.1016/j.ecolind.2021.108351>, 2021.
- 600 Reichstein, M., Falge, E., Baldocchi, D., Papale, D., Aubinet, M., Berbigier, P., Bernhofer, C., Buchmann, N., Gilmanov, T., Granier, A., Grünwald, T., Havráňková, K., Iivesniemi, H., Janous, D., Knohl, A., Laurila, T., Lohila, A., Loustau, D., Matteucci, G., Meyers, T., Miglietta, F., Ourcival, J., Pumpanen, J., Rambal, S., Rotenberg, E., Sanz, M., Tenhunen, J., Seufert, G., Vaccari, F., Vesala, T., Yakir, D., and Valentini, R.: On the separation of net ecosystem exchange into assimilation and ecosystem respiration: review and improved algorithm, *Global Change Biology*, 11, 1424–1439, <https://doi.org/10.1111/j.1365-2486.2005.001002.x>, 2005.
- Schmid, H. P.: Footprint modeling for vegetation atmosphere exchange studies: a review and perspective, *Agricultural and Forest Meteorology*, 113, 159–183, [https://doi.org/10.1016/S0168-1923\(02\)00107-7](https://doi.org/10.1016/S0168-1923(02)00107-7), 2002.
- 605 Tyrälis, H. and Papacharalampous, G.: Variable Selection in Time Series Forecasting Using Random Forests, *Algorithms*, 10, 114, <https://doi.org/10.3390/a10040114>, 2017.
- Vesala, T., Kljun, N., Rannik, Ü., Rinne, J., Sogachev, A., Markkanen, T., Sabelfeld, K., Foken, Th., and Leclerc, M. Y.: Flux and concentration footprint modelling: State of the art, *Environmental Pollution*, 152, 653–666, <https://doi.org/10.1016/j.envpol.2007.06.070>, 2008.
- 610 Wang, S., Chen, W., Fu, Z., Li, Z., Wang, J., Liao, J., and Niu, S.: Seasonal and Inter-Annual Variations of Carbon Dioxide Fluxes and Their Determinants in an Alpine Meadow, *Front. Plant Sci.*, 13, 894398, <https://doi.org/10.3389/fpls.2022.894398>, 2022.
- 615 Wang, X., Wang, T., Liu, D., Zhang, T., Xu, J., Cui, G., Lv, G., and Huang, H.: Multisatellite Analyses of Spatiotemporal Variability in Photosynthetic Activity Over the Tibetan Plateau, *JGR Biogeosciences*, 124, 3778–3797, <https://doi.org/10.1029/2019JG005249>, 2019.
- Wang, Y. and Ma, Y.: Spatio-temporal patterns of NEE based on upscaling eddy covariance measurements in the alpine grassland of the Tibetan Plateau, *display*, <https://doi.org/10.5194/egusphere-egu22-1440>, 2022.
- 620 Wang, Y., Ma, Y., Li, H., and Yuan, L.: Carbon and water fluxes and their coupling in an alpine meadow ecosystem on the northeastern Tibetan Plateau, *Theor Appl Climatol*, 142, 1–18, <https://doi.org/10.1007/s00704-020-03303-3>, 2020.
- Wang, Y., Xiao, J., Ma, Y., Luo, Y., Hu, Z., Li, F., Li, Y., Gu, L., Li, Z., and Yuan, L.: Carbon fluxes and environmental controls across different alpine grassland types on the Tibetan Plateau, *Agricultural and Forest Meteorology*, 311, 108694, <https://doi.org/10.1016/j.agrformet.2021.108694>, 2021.
- 625 Wei, D., Qi, Y., Ma, Y., Wang, X., Ma, W., Gao, T., Huang, L., Zhao, H., Zhang, J., and Wang, X.: Plant uptake of CO₂ outpaces losses from permafrost and plant respiration on the Tibetan Plateau, *Proc. Natl. Acad. Sci. U.S.A.*, 118, e2015283118, <https://doi.org/10.1073/pnas.2015283118>, 2021.
- Wutzler, T., Lucas-Moffat, A., Migliavacca, M., Knauer, J., Sickel, K., Šigut, L., Menzer, O., and Reichstein, M.: Basic and extensible post-processing of eddy covariance flux data with REddyProc, *Biogeosciences*, 15, 5015–5030, <https://doi.org/10.5194/bg-15-5015-2018>, 2018.
- 630 Yun, H., Tang, J., D’Imperio, L., Wang, X., Qu, Y., Liu, L., Zhuang, Q., Zhang, W., Wu, Q., Chen, A., Zhu, Q., Chen, D., and Elberling, B.: Warming and Increased Respiration Have Transformed an Alpine Steppe Ecosystem on the Tibetan Plateau From a Carbon Dioxide Sink Into a Source, *JGR Biogeosciences*, 127, e2021JG006406, <https://doi.org/10.1029/2021JG006406>, 2022.
- 635 Zhang, T., Zhang, Y., Xu, M., Zhu, J., Chen, N., Jiang, Y., Huang, K., Zu, J., Liu, Y., and Yu, G.: Water availability is more important than temperature in driving the carbon fluxes of an alpine meadow on the Tibetan Plateau, *Agricultural and Forest Meteorology*, 256–257, 22–31, <https://doi.org/10.1016/j.agrformet.2018.02.027>, 2018.



Zhao, S. and Liu, S.: Scale criticality in estimating ecosystem carbon dynamics, *Global Change Biology*, 20, 2240–2251, <https://doi.org/10.1111/gcb.12496>, 2014.

640 Zheng, Y., Liu, H., Du, Q., Liu, Y., Sun, J., Cun, H., and Järvi, L.: Effects of precipitation seasonal distribution on net ecosystem CO₂ exchange over an alpine meadow in the southeastern Tibetan Plateau, *Int J Biometeorol*, 66, 1561–1573, <https://doi.org/10.1007/s00484-022-02300-7>, 2022.

Zhu, Z., Ma, Y., Li, M., Hu, Z., Xu, C., Zhang, L., Han, C., Wang, Y., and Ichiro, T.: Carbon dioxide exchange between an alpine steppe ecosystem and the atmosphere on the Nam Co area of the Tibetan Plateau, *Agricultural and Forest Meteorology*, 203, 169–179, <https://doi.org/10.1016/j.agrformet.2014.12.013>, 2015.